J Mater Sci (2007) 42:252–258
DOI 10.1007/s10853-006-1061-0

Synthesis of pure Zn_2SiO_4:Mn green phosphors by simple PVA–metal complex route

A. Manavbasi · J. C. LaCombe

Received: 16 June 2005 / Accepted: 4 January 2006 / Published online: 28 November 2006

Abstract Green light emitting $Zn_{2-x}Mn_xSiO_4$ (willemite) particles were synthesized by a simple and cost-effective poly(vinyl alcohol) (PVA)-complex route. Microstructural studies on the calcined products show that particles are pure, single phase, nano-crystalline, and agglomerated morphology. A pure-phase willemite structure was obtained with calcination between 850 and 1,175 °C for 2 h in air. Particle size analysis indicates that the average particle size is ~1 μm. The photoluminescence properties of these 4 and 12 mol% Mn-doped Zn_2SiO_4 powders were measured by fluorescence spectroscopy. Particles with 4 mol% Mn doping prepared at 1,150 °C, with an emission decay time, I_0/e, of 13.4 ms showed the highest relative peak emission intensities. The emission intensity at this doping level was measured to be ~110% of a representative commercial product's, doped with 11.2 mol% Mn, and exhibiting a decay time of 7.1 ms. The effect of calcination temperature on the photoluminescence and crystallinity properties of synthesized green powders was also investigated.

Introduction

The manganese-doped zinc orthosilicate $Zn_{2-x}Mn_xSiO_4$ is used as a green luminescent phosphor in cathode ray tubes, lamps, and plasma display panels because of its high saturated color, very strong luminescence, long life span, lack of moisture sensitivity, and chemical stability [1–3]. Zn_2SiO_4:Mn was also found to be a promising alternative to the conventional thin film phosphors in electroluminescent devices [4], and appropriate for medical imaging detectors for low-voltage radiography and fluoroscopy [5, 6].

The photoluminescence properties of phosphors mainly depend on the dopant choice and composition, the choice of host lattice, and the synthesis methods used. The conventional method to synthesize Zn_2SiO_4:Mn phosphor is the solid-state reaction which requires high firing temperatures and a milling process as a post-treatment method. This mechano-chemical activation process generates largely agglomerated and irregular particles with relatively weak luminescence properties [7]. For this reason, in the last two decades, much effort has been dedicated to synthesize Zn_2SiO_4:Mn phosphors with new methods such as sol–gel [8–10], concentration gradient uniform particle size [11], hydrothermal [12], spray pyrolysis [2, 13], fume pyrolysis [14], polymer pyrolysis [15], and combustion synthesis [16]—each method producing material with the desirable luminescence. Although several chemical methods have been applied to the production of fine phosphor particles with good luminescence, challenges remain in reducing process complexity, controllability, and cost. Therefore, new synthesis routes are being explored to potentially overcome some of these difficulties in commercialization. During recent years, novel organic–inorganic polymerization synthesis routes have been applied to produce a variety of mixed oxide metals. For example, poly(vinyl alcohol) (PVA) $-[CH_2-CHOH]-_n$ and poly(ethylene glycol) (PEG) $H[O-CH_2-CH_2]_n-OH$ have been

A. Manavbasi · J. C. LaCombe (✉)
Metallurgical and Materials Engineering, University of Nevada, 1664 North Virginia St, Mail Stop 388, Reno, NV 89557, USA
e-mail: lacomj@unr.edu

reported for use in synthesis as an organic component, with water dissoluble metal cations added as the inorganic component [17–21].

In this study, manganese doped willemite, Zn_2SiO_4:Mn, green phosphor particles were produced by a simple PVA–metal complex route. The photoluminescence properties, crystallinity, particle size, and morphology were investigated, with the results reported here.

Experimental procedure

The synthesis process used in this work involves preparation of cationic precursors and mixing them with a viscous PVA–H_2O solution. This is then heated to evaporate the water, leaving behind an intermediate powder which is calcined at elevated temperature to significantly improve purity and crystallinity, and create uniform doping in the resulting phosphor powders. All polymeric and cationic solutions were prepared fresh. This process is described more fully below.

The PVA–metal complex precursor for $Zn_{2-x}Mn_xSiO_4$ was prepared using $Zn(NO_3)_2 \cdot 6H_2O$ (99%, Alfa Aesar), $Mn(NO_3)_2 \cdot 4.4H_2O$ (99.98%, Alfa Aesar), Ludox TMA colloidal silica solution (ChemPoint.com) with an average colloidal particle size of 5.78 nm, and PVA (molecular weight of 145,000) with degree of polymerization of 3300 (Sigma-Aldrich Inc.). According to the PVA's product specifications, the nominal ''100 mol% hydrolyzed PVA'' actually contains up to 2 mol% of acetate groups, which replace the OH–cation bonds used in our process. Thus, in our calculations, we assumed an average 99 mol% degree of hydrolysis.

Synthesis begins with a 5 wt.% PVA–H_2O solution, prepared on a hot plate at ~85 °C (with mixing) until a clear viscous solution results. Stoichiometric amounts of the cationic nitrates were dissolved in the minimal necessary amount of D.I. water by stirring in a separate container at room temperature and then added to the heated PVA–H_2O aqueous solution. Typically, 120 g batches of the PVA–metal solution were prepared for each set of conditions. The proportions of the PVA and cation sources in the precursor solution were adjusted to provide a targeted PVA monomer unit:metal ion mole ratio of 2:1 to ensure sufficient hydroxyl (OH^-) groups were available for cation dispersion in the PVA. Ideally, this helps avoid cation (metal) precipitation and agglomeration. Each monomer part of the long PVA polymeric chains has one hydroxyl group in the aqueous solution and the relative stoichiometric values of the cations in the solution were calculated based on the total number of hydroxyl functional groups, given the solution concentration, degree of hydrolysis, and degree of polymerization. The PVA–metal aqueous solution was then heated on a hot plate at a temperature of ~150 °C with continuous mixing. After evaporation (8–10 h), a dark brown, soft, loosely connected precursor powder typically remains. Each sample powder batch (typically 0.2 g after evaporation) was calcined in air at different temperatures up to 1,175 °C, for a fixed 2-h period and then air cooled to obtain the final manganese-doped green phosphors.

The crystallization behavior and the crystallite size measurements of the phosphors were studied via room temperature X-ray diffraction (XRD) as a function of the calcination temperature using a Philips P.W. 2273/20 diffractometer with Cu Kα radiation (45 kV, 30 mA). The particle sizes and size distributions were measured using a Microtrac® Nanotrac NPA 250 particle size analyzer. For the particle size measurements, powders were dispersed in 20 wt.% glycerin–D.I. water solution, via ultrasonication. Photoluminescence characteristics in the visible range were recorded on a Hitachi F-4500 fluorescence spectrophotometer with a 150 W Xe lamp, using a 254 nm (ultraviolet) excitation wavelength. Decay time measurements were performed via time-resolved spectroscopy with the same equipment. Scanning electron microscopy (SEM) was conducted using a Hitachi S-4700 cold field emission SEM, with the powder samples coated with Pt. Mn dopant levels in a commercial powder (evaluated to serve as a baseline comparison) were measured using a Perkin-Elmer 2380 Atomic Absorption Spectrophotometer.

Using the above-described procedures, we prepared a set of powders at two different manganese doping concentrations (4 and 12 mol%) and examined a range of calcination temperatures between 750 and 1,175 °C to determine the influence these parameters had on the material properties. Comparisons were made with a commercially available Zn_2SiO_4:Mn product provided by OSRAM SYLVANIA Products Inc.

Results and discussion

XRD analysis

XRD patterns for 4 mol% Mn doped Zn_2SiO_4 phosphors, measured from samples calcined at various temperatures (as well as the commercial phosphor) are shown in Fig. 1. The as-synthesized powders and those

calcined at 750 °C showed unreacted ZnO peaks near $2\theta = 36°$ with an amorphous structure. Single phase zinc orthosilicate crystal structures with similar crystallinity (i.e., the willemite phase, exhibiting the phenacite structure) to that of the commercial powder, start to form at calcination temperatures of ~850 °C after 2 h. The Mn doping concentration in the commercial phosphor was measured to be 11.2 mol% using atomic absorption spectroscopy, which is close to the composition of a commercial product Zn_2SiO_4:Mn reported elsewhere [22] (~10 mol%). All powders had a white color, indicative that the manganese is in the desired Mn^{2+} state [3] after heat treating at (and above) 950 °C. Other reports [1], indicate that synthesis using solid-state and solution reaction methods yielded the same single-phase willemite at 1,400 °C (for 4 h) and 1,200 °C (for 4 h), respectively. The spray pyrolysis method [13], has been reported to give the same phase at 1,200 °C (for 5 h). Combustion synthesis [16] and the hydrothermal method [12], resulted in single-phase willemite without any high temperature heat treatment.

The peak positions in Fig. 1 match well with those of the standard pattern (JCPDS 37-1485) for Zn_2SiO_4 in the phenacite structure. In order to investigate the crystallinity dependence on the calcination temperatures, the FWHM values of the main peaks were measured and found to decrease from 0.30° to 0.24° as the temperature increased from 950 to 1,175 °C. Also, the peak intensities increased with increasing calcination temperatures leading to the conclusion that the crystallinity of phosphor particles was increased with calcination temperature. Individual crystallite sizes were estimated using Scherrer's formula and were found to shift from ~25 to ~38 nm as the temperature was increased from 850 to 1,175 °C.

Photoluminescence spectra characterization

Emission spectra (under 254 nm excitation) for phosphor particles prepared at various calcination temperatures are shown in Fig. 2. As the temperature increases, the emission peak intensity increases, with the highest intensities obtained in the 1,160–1,175 °C range. These intensities were ~120% that of the commercial product's particles. Phosphors (5 mol% Mn) prepared with spray pyrolysis [13] at 800 °C and post-treated at 1,100 °C reportedly had an intensity maximum of ~112% of the commercial product. As the manganese content is increased from 4 to 12 mol%, the maxima of the emission band was observed to shift slightly to a higher wavelength, from 523 to 526 nm, and with a bandwidth change of $\Delta\lambda$ = 38 nm to 39 nm at half maximum, respectively. These characteristic wavelength values are attributed to the presence of Mn^{2+} cations in the willemite structure. Both Zn^{2+} and Si^{4+} ions coordinate tetrahedrally with four oxygen atoms in the Zn_2SiO_4 crystal lattice [23], and in this host lattice, Mn^{+2}, with a weak crystal field, usually gives green emission. There are reportedly two different Zn sites with nearest oxygen ions in a slightly distorted tetrahedral configuration [24]. As the difference in ionic radii of Zn^{2+} (0.074 nm) and Mn^{2+} (0.080 nm) is very small, both Zn^{2+} sites can be replaced by Mn^{2+} ions [25]. The Mn^{2+} ion has $3d^5$ configuration with high spin and the emission band is assigned to transition from the lowest excited state $^4T_1$ to the ground state $^6A_1$ [23, 24].

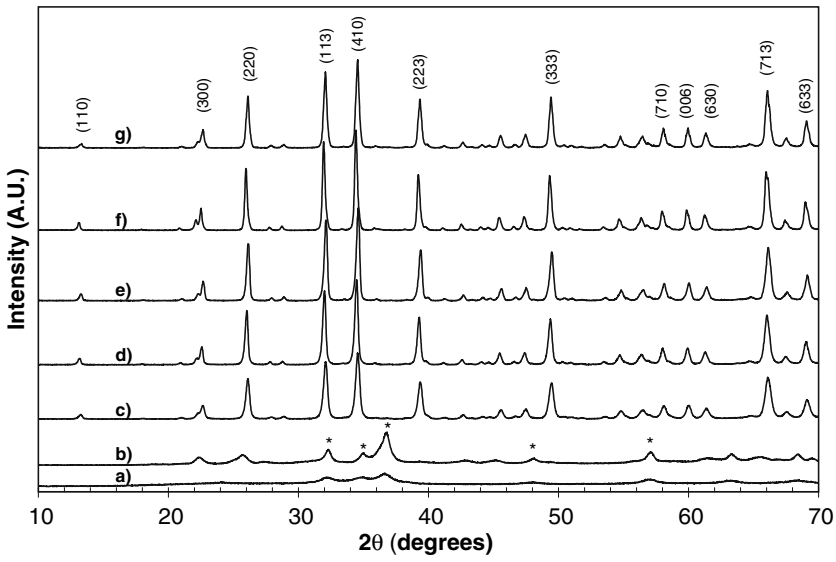

Fig. 1 X-ray diffraction spectra for 4 mol% Mn doped $Zn_{2-x}Mn_xSiO_4$ prepared for 2 h at various temperatures and the commercial one. Conditions are as follows: (**a**) as–synthesized, (**b**) 750 °C, (**c**) 850 °C, (**d**) 950 °C, (**e**) 1,050 °C, (**f**) 1,150 °C, and (**g**) commercial powder. (*: ZnO). Note that at temperatures above ~850 °C, crystallinity is significantly improved, and the primary ZnO peak disappears, suggesting a predominantly single-phase willemite material

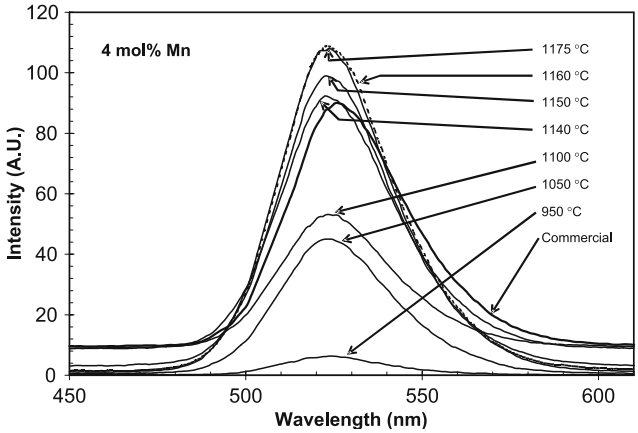

Fig. 2 Emission spectra (excited at 254 nm) of 4 mol% Mn doped Zn_2SiO_4:Mn phosphor particles calcined at different temperatures for 2 h in air, including a commercially available sample with 11.2 mol% Mn doping. Most efficient emission occurs in the higher calcination temperature powders

Zn^{2+} exhibits an intense and broad UV absorption in the short wavelength, an energy transfer to Mn^{2+} takes place, resulting in the green emission from the Zn_2SiO_4:Mn phosphor [23, 26]. The UV absorption–transition process has been suggested [23] to include a charge transfer transition from the 2p orbital of oxygen to an anti-bonding orbital, which is localized partly on the d^{10} level of the Zn^{2+} ion and partly on the 2p level of the oxygen.

Figure 3 shows the excitation spectrum for 4 and 12 mol% Mn doped samples calcined at 1,160 °C for 2 h, and the commercial powder with 11.2 mol% Mn.

Figure 4 shows the observed relative peak emission intensities of 4 and 12 mol% Mn doped Zn_2SiO_4:Mn samples at various calcination temperatures ranging from 950 to 1,175 °C. For both measured concentration

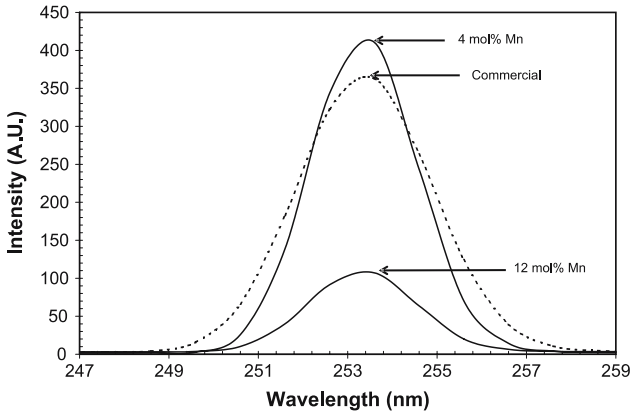

Fig. 3 Excitation spectra of 4 and 12 mol% Mn doped samples prepared at 1,160 °C for 2 h, and commercial (11.2 mol%) Zn_2SiO_4:Mn phosphor, all excited at 254 nm

levels, the emission intensity was increased sharply when the calcination temperatures increased. The peak emission intensity of the 4 mol% Mn doped phosphor prepared at 1,175 °C is almost 17 times higher than that of phosphors prepared at 950 °C. Overall, phosphors with 4 mol% Mn showed higher emission intensities than those doped with 12 mol% Mn. This behavior has been attributed to the concentration quenching phenomenon [24].

When the Mn^{2+} dopant concentration increased, there is expected to be energy transfer between Mn^{2+}–Mn^{2+} ions [24]. This can take excitation energy too far from the absorption location, potentially losing the excitation at a quenching site, without any photon radiation and lead to a decrease in luminescence efficiency [23, 24]. At low concentrations of Mn^{2+} ions, the concentration quenching effect is negligible because the average distance between Mn^{2+} ions is relatively large and the energy migration is prevented.

SEM characterization

Scanning electron microscope (SEM) images for the as-synthesized powders and the 4 mol% Mn doped samples prepared at 1,150 °C for 2 h are illustrated in Fig. 5. Micrographs show that the as-synthesized particles are highly agglomerated at the micron-scale.

Additionally, the calcined phosphor particles have an irregularly rounded morphology and solid-filled

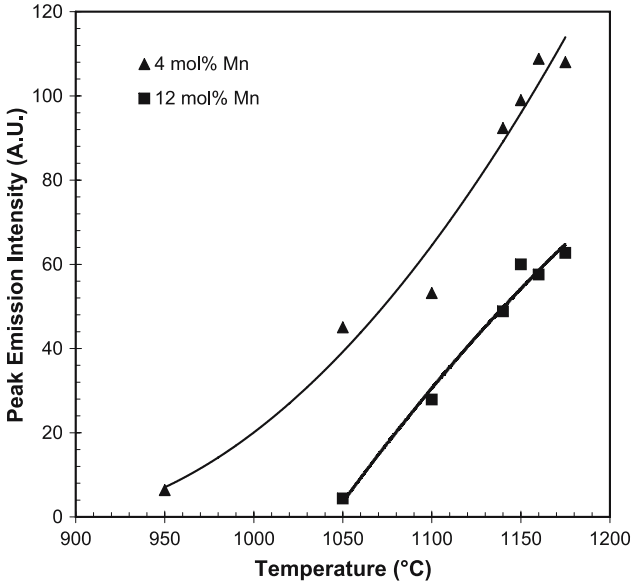

Fig. 4 Comparison of peak emission intensity in 4 and 12 mol% Mn doped Zn_2SiO_4:Mn phosphors as a function of the calcination temperatures. Excitation was done at 254 nm. The trend of more efficient emission with increasing calcination temperature is clear

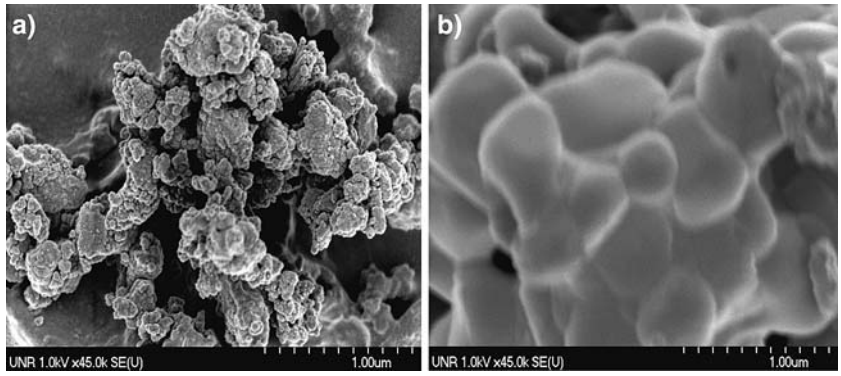

Fig. 5 SEM micrographs of 4 mol% Mn doped powder samples: (**a**) as-synthesized and (**b**) calcined at 1,150 °C for 2 h in air. Agglomerations of smaller particles (which XRD indicates consist of still-smaller grains) are shown

structure without any porosity in the range of 200–500 nm. These sub-micron particles formed irregularly rounded aggregates in micron size.

Particle size measurements

A typical particle size distribution for phosphor particles calcined at 1,150 °C is shown in Fig. 6. Phosphor particles were dispersed in 20 wt.% glycerin–water solution by ultrasonication prior to particle size analysis. The average discrete particle size is ~1 μm, with a range of sizes extending from 200 nm to 4 μm for all measured manganese doping levels.

Decay time measurements

It is widely accepted that photoluminescent properties of phosphors can depend on their shape, size, and surface texture, as well as the composition. These properties of the phosphors should be optimized to obtain the maximum quantum efficiency through energy absorption [1]. The intensity decay of a photoluminescence process can be expressed in the functional form: $I_{em} = I_0 e^{-t/\tau}$, where the lifetime τ refers to the time required for the intensity to drop to I_0/e [27].

Figure 7 shows the measured intensity decay plots, including the measured lifetimes to reach intensities of I_0/e and $I_0/10$. Phosphors calcined at 1,150 °C and doped with 4 mol% Mn decayed to I_0/e in 13.4 ms and $I_0/10$ in 31.2 ms. The 12 mol% Mn phosphor (also calcined at 1,150 °C) decayed to I_0/e in 5.0 ms and $I_0/10$ in 11.2 ms.

Similarly, the decay times for the commercial product we evaluated were found to be 7.1 ms at I_0/e, and 13.5 ms at $I_0/10$, placing the commercial product's decay times in between the 4 and 12 mol% samples produced in this effort.

Similar comparisons have been made in the literature, which report that the decay times measured at $I_0/10$, (i.e., $\tau_{10\%}$), typically fall in the range

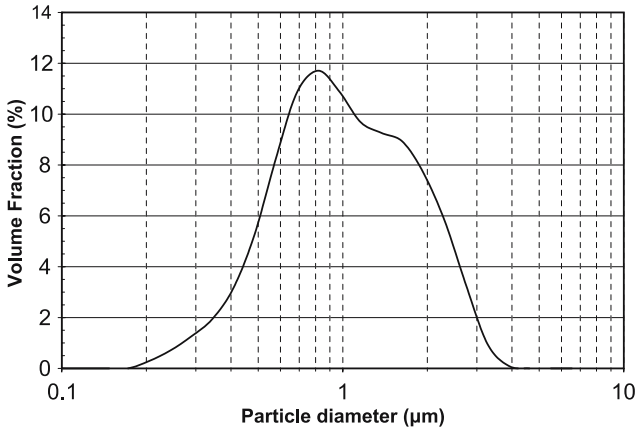

Fig. 6 Particle size distribution of 4 mol% Mn doped Zn_2SiO_4:Mn phosphors calcined at 1,150 °C for 2 h in air. The size distribution is fairly large (200 nm to 3 μm), with a mean diameter of ~1 μm

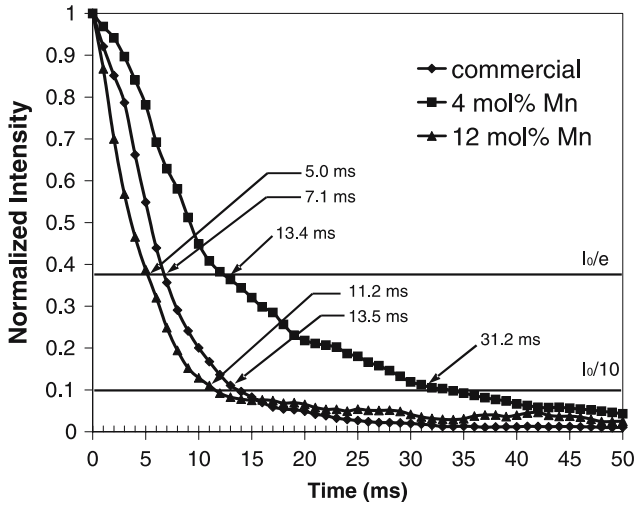

Fig. 7 Decay curves of $Zn_{2-x}Mn_xSiO_4$ phosphors with 4 and 12 mol% Mn doping levels, as well as a commercial product (11.2 mol% Mn) shown for comparison

of 5–25 ms [1–3, 22] at the same Mn doping levels. The emission decay time behavior is reported to be dictated by the energy migration between proximate manganese ions [24]. Thus, the Mn doping level can be expected to influence the diffusion-controlled emission decay time. The decay times for the phosphors produced here extend from as short as 5 ms, to over 31 ms. This overlaps the range of values reported elsewhere in the literature, as well as the commercial product included in this study. Whereas it was found in this effort that the decay time can be varied over a range, a systematic study of this behavior was beyond the scope of this effort. The range of decay times achieved here suggest that phosphors with decay times of 5–10 ms and very bright emission intensities, can likely be achieved simply through doping concentration. In general, additional studies would be needed to determine whether other controllable parameters would impact the photoluminescence behavior of these phosphors. Examples of potential utility include the degree of PVA polymerization, the degree of hydrolysis of the PVA, cation source selection, the mole ratio of PVA monomer to metal cations, and the use of different polymerizing and combustion agents.

Conclusions

Green light emitting Zn_2SiO_4:Mn phosphor particles with rounded and filled morphologies without any porosity, and with good luminescence properties were produced using a simple PVA–metal complex route. This method requires a short thermal processing time of 2 h in air at a minimum temperature of 950 °C. This results in phosphors with the desired willemite phase, and with Mn-doping in the desired Mn^{2+} state yielding green light emission under 254 nm UV excitation. In general, as the calcination temperature is increased (within the range investigated here), we found the emission intensity to increase (within the <1,175 °C range that was investigated here). The photoluminescence data revealed that the 4 mol% Mn doped samples prepared in the calcination temperature range of 1,150–1,175 °C showed very high emission peak intensities compared to the 12 mol% Mn doped samples. This 4 mol% Mn doped material also exhibited emission intensities that were 110–120% that of the tested commercially available product. The calcined samples exhibit irregularly rounded particles of 200–500 nm size, agglomerated into an overall average particle size of ~1 μm for samples prepared at both manganese doping levels, i.e., the agglomeration behavior was insensitive to doping composition in the range of composition evaluated here. Highly crystalline phosphor particles without any porosity and with smooth, rounded surface texture are demonstrated here to give good luminescence properties in comparison with available commercial products, complementing the simple and reliable synthesis process used in their creation.

The data presented here indicate that there may be some potential for the application of a relatively simple PVA–metal complex synthesis method to produce phosphor materials such as the green phosphor, Zn_2SiO_4:Mn. Further development of this synthesis method for application in different phosphor systems is presently under way.

Acknowledgements The authors wish to thank Dr. O. Graeve for technical assistance and access to photoluminescence and particle size analysis equipment, M. Ahmadiantehrani for SEM support, and ChemPoint.com for colloidal silica solutions. We also wish to thank OSRAM SYLVANIA Products Inc. for providing commercially available material for comparison purposes described herein.

References

1. Cho TH, Chang HJ, (2003) Ceram Int 29: 611
2. Kang YC, Park HD, (2003) Appl Phys A 77: 529
3. Morell A, Khiati NE, (1993) J Electrochem Soc 147(7):2019
4. Xiao T, Liu G, Adams M, Kitai AH, (1996) Can J Phys 74: 132
5. Cavouras D, Kandarakis I, Nomicos CD ,Panayiotakis GS, Fezoulidis I (2000) Appl Radiat Isot 52: 119
6. Kandarakis I, Cavouras D, Prassopoulos P, Kanellopoulos E, Nomicos CD, Panayiotakis GS (1998) Appl Phys A 67: 521
7. Sohn KS ,Cho B, Park HD (1999) J Am Ceram Soc 82: 2779
8. Morimo R, Matae K (1989) Mater Res Bull 24(2): 175
9. Thristov TI ,Popvich NV ,Galaktionov SS, Soschin NP (1996) Inorg Mater 32(1):80
10. Reynaud L, Cabarrecq CB ,Mosset A, Ahamdane H (1996) Mater Res Bull 31(9): 1133
11. Chang IF, Brownlow JESJW (1989) J Electrochem Soc 136(11): 3532
12. Yoon C, Knag S (2001) J Mater Res 16(4): 1210
13. Kang YC, Park SB (2000) Mater Res Bull 35: 1143
14. Morimo R, Monchinaga R, Nakamura K (1994) Mater Res Bull 29(7): 751
15. Su K, Tiley TD, Sailor MJ (1996) J Am Chem Soc 118: 3459
16. Bhatkar VB ,Omanwar SK, Moharil SV (2002) Phys Stat Sol 191(1): 272
17. Pramanik P, Pathak A (1994) Bull Mater Sci 17(6): 967
18. Saha SK ,Pathak A, Pramanik P (1995) J Mater Sci Lett 14: 35
19. Gulgun MA ,Nguyen MH, Kriven WM (1999) J Am Ceram Soc 82(3): 556

20. Lee SJ ,Lee CH, Kriven WM (2000) J Ceram Proc Res 1(2): 92
21. Gulgun MA ,Kriven WM, Nguyen MH (2002) Processes for preparing mixed metal oxide powders, US Patent 6,482,387 (WM Kriven, USA, 2002)
22. Kim KN ,Jung HK, Park HD (2002) J Lumin 99: 169
23. Blasse G, Grabmaier BC (1994) Luminescent materials. Springer-Verlag, Berlin
24. Barthou C, Benoit J, Benalloul P, Morell A (1994) J Electrochem Soc 141(2): 524
25. Perkins HK, Sienko MJ (1967) J Chem Phys 46(6): 2398
26. Jenkins HG, Mckeag AH, Rooksby (1939) HP Nature 143: 978
27. Pringsheim P (1949) Fluorescence phosphorescence. Interscience Publishers Inc., New York